

Diffusion entropy and waiting time statistics of hard x-ray solar flares

Paolo Grigolini^{1,2,3}, Deborah Leddon¹, Nicola Scafetta¹

¹*Center for Nonlinear Science, University of North Texas, P.O. Box 305370, Denton, Texas 76203*

²*Dipartimento di Fisica dell'Università di Pisa, Piazza Torricelli 2, 56127 Pisa, Italy*

³*Istituto di Biofisica del Consiglio Nazionale delle Ricerche, Via San Lorenzo 26, 56127 Pisa, Italy*

(October 26, 2018)

We analyze the waiting time distribution of time distances τ between two nearest-neighbor flares. This analysis is based on the joint use of two distinct techniques. The first is the direct evaluation of the distribution function $\psi(\tau)$, or of the probability, $\Psi(\tau)$, that no time distance smaller than a given τ is found. We adopt the paradigm of the inverse power law behavior, and we focus on the determination of the inverse power index μ , without ruling out different asymptotic properties that might be revealed, at larger scales, with the help of richer statistics. The second technique, called Diffusion Entropy (DE) method, rests on the evaluation of the entropy of the diffusion process generated by the time series. The details of the diffusion process depend on three different walking rules, which determine the form and the time duration of the transition to the scaling regime, as well as the scaling parameter δ . With the first two rules the information contained in the time series is transmitted, to a great extent, to the transition, as well as to the scaling regime. The same information is essentially conveyed, by using the third rules, into the scaling regime, which, in fact, emerges very quickly after a fast transition process. We show that the significant information hidden within the time series concerns memory induced by the solar cycle, as well as the power index μ . The scaling parameter δ becomes a simple function of μ , when memory is annihilated. Thus, the three walking rules yield a unique and precise value of μ if the memory is wisely taken under control, or cancelled by shuffling the data. All this makes compelling the conclusion that $\mu = 2.138 \pm 0.01$.

05.40.Fb, 05.45.Tp, 96.60.Rd, 89.90.+n

I. INTRODUCTION

The study of solar flares is becoming popular among the researchers working at the frontier of statistical mechanics, due to the widely shared conviction that they are a signature of a significant departure from the condition of ordinary Brownian motion [1–4]. As pointed out by Wheatland, [5], the distribution of times between flares, gives information on how to model flare statistics. In this paper we shall be referring to these times, denoted by us with the symbol τ , as the time distance between two consecutive events and the corresponding distribution density will be denoted by $\psi(\tau)$. Although the agreement on the fact that flare statistics depart from ordinary statistical mechanics is general, there seems to be the still unsettled issue of what is the proper model which will account for this form of anomalous statistics. Does this form of statistics reflect self-organized criticality or turbulence [3]? We think that the settlement of this delicate issue is made difficult by the fact that, although many authors claim that $\psi(\tau)$ is an inverse power law with power index μ , the actual value of μ still seems to be uncertain. In fact, the authors of Ref. [1] propose $\mu = 1.7$ and those of Ref. [2] claim that $\mu = 2$ is the proper power law index. Boffetta et al. [3] propose $\mu = 2.4$. Finally, Wheatland explains the origin of the power law behavior with a model yielding $\mu = 3.0$, [5].

As it will be made clear by the theoretical analysis of this paper, it is possible to prove, without taking position on the origin of the inverse power law behavior, that $\mu = 3$ and $\mu = 2$ are critical values. In fact, we note that

moving from $\mu > 3$ to $\mu < 3$ is equivalent to a phase transition from the Gaussian to the Lévy basin of attraction [6], and moving from $\mu > 2$ to $\mu < 2$ implies a transition from the condition of Lévy statistics to a form of out of equilibrium regime [7]. Thus, an uncertainty larger than the distance of the border $\mu = 2$ from the border $\mu = 3$ is judged by us to be an unsatisfactory condition that might delay the settlement of the issues concerning the complex dynamics underlying the waiting time statistics. The main purpose of this paper is to illustrate a statistical method of analysis that yields a reliable value for the power index μ . We hope that this result might be useful for the researchers in this interesting field of investigation and at the same time might be beneficial in general for all those who are interested in the statistical analysis of time series.

The outline of the paper is as follows. In Section II we review the method of Diffusion Entropy (DE) that will be a crucial step of the statistical analysis done in this paper. Although the method has been applied somewhere else [8–10], we will present a short review in order to make this paper as self-contained as possible. In Section III, we illustrate a dynamical model that in general results in time sequences that are statistically equivalent to those observed in real data. This model is not limited to the case of inverse power laws, but here we make the assumption that the shifted inverse power law is an ideal condition convenient to analyze solar flares, and we study the explicit form emerging from this condition. In Section IV, we illustrate two walking prescriptions that will be used to convert the real data into random trajectories.

The benefit of adopting several walking prescriptions was discussed in Ref. [9]. Here we introduce two new rules and we apply both of them as well as one of those introduced in Ref. [9]. In Section V we prove that the numerical evaluation of the probability of getting a waiting time larger than a given τ yields a value for μ more accurate than that afforded by the waiting-time distribution $\psi(\tau)$. In Section VI we show how to process the data to make an efficient use of the DE method. In Section VII we use the DE method to further reduce the error of Section V. We devote Section VIII to concluding remarks.

II. DIFFUSION ENTROPY

The main idea of this approach to scaling is remarkably simple. Let us consider a sequence of M numbers, $\xi_i(t)$, with $i = 1, \dots, M$. The purpose of the DE algorithm is to establish the possible existence of a scaling, either normal or anomalous, in the most efficient way as possible without altering the data with any form of detrending. Let us select first of all an integer number l , fitting the condition $1 \leq l \leq M$. This integer number will be referred to by us as “time”. For any given time l we can find $M - l + 1$ sub-sequences defined by

$$\xi_i^{(s)} \equiv \xi_{i+s}, \quad s = 0, \dots, M - l. \quad (1)$$

For any of these sub-sequences we build up a diffusion trajectory, labeled with the index s , defined by the position

$$x^{(s)}(l) = \sum_{i=1}^l \xi_i^{(s)} = \sum_{i=1}^l \xi_{i+s}. \quad (2)$$

Let us imagine this position as referring to a Brownian particle that at regular intervals of time has been jumping forward or backward according to the prescription of the corresponding sub-sequence of Eq.(1). This means that the particle before reaching the position that it holds at time l has been making l jumps. The jump made at the i -th step has the intensity $|\xi_i^{(s)}|$ and is forward or backward according to whether the number $\xi_i^{(s)}$ is positive or negative.

We are now ready to evaluate the entropy of this diffusion process. To do that we have to partition the x -axis into cells of size $\epsilon(l)$. When this partition is made we have to label the cells. We count how many particles are found in the same cell at a given time l . We denote this number by $N_i(l)$. Then we use this number to determine the probability that a particle can be found in the i -th cell at time l , $p_i(l)$, by means of

$$p_i(l) \equiv \frac{N_i(l)}{(M - l + 1)}. \quad (3)$$

At this stage the entropy of the diffusion process at time l is determined and reads

$$S_d(l) = - \sum_i p_i(l) \ln[p_i(l)]. \quad (4)$$

The easiest way to proceed with the choice of the cell size, $\epsilon(l)$, is to assume it to be independent of l and determined by a suitable fraction of the square root of the variance of the fluctuation $\xi(i)$. In the case in which the numbers ξ_i are $+1$, 0 and -1 , $\epsilon = 1$ is the natural choice.

Before proceeding with the illustration of how the DE method works, it is worth making a comment on how to define the trajectories. The method we are adopting is based on the idea of a moving window of size l that makes the $s - th$ trajectory closely correlated to the next, the $(s + 1) - th$ trajectory. The two trajectories have $l - 1$ values in common. It is worth making a comparison with the technique of Detrended Fluctuation Analysis (DFA) [11]. The DFA is a popular method of scaling analysis, aiming at detecting the long-range correlations in seemingly non-stationary time series that in the last few years has been used in more than 100 publications [12]. The DFA is based on non-overlapping windows, and, consequently, trajectories with different labels are totally independent from one another. The motivation for using overlapping windows, with the DE method, is given by our wish to establish a connection with the Kolmogorov-Sinai (KS) entropy [13,14]. In Section III we shall make further comments on this connection. The KS entropy of a symbolic sequence is evaluated by moving a window of size l along the sequence. Any window position corresponds to a given combination of symbols, and from the frequency of each combination it is possible to derive the Shannon entropy $S(l)$. The KS entropy is given by the asymptotic limit $\lim_{l \rightarrow \infty} S(l)/l$. We believe that the same sequence, analyzed with the DE method, at the large values of l where a finite KS entropy shows up, must yield a well defined scaling δ . To realize this correspondence we carry out the determination of the DE by using the same criterion of overlapping windows as that behind the KS entropy.

Details on how to deal with the transition from the short-time regime, sensitive to the discrete nature of the process under study, to the long-time limit where both space and time can be perceived as continuous, are given in Ref. [10]. Here we make the simplifying assumption of considering large enough times as to make the continuous assumption valid. In this case, the trajectories, built up with the above illustrated procedure, correspond to the following equation of motion:

$$\frac{dx}{dt} = \xi(t), \quad (5)$$

where $\xi(t)$ denotes the value that the time series under study gets at the $l - th$ site of the sequence under study. This means that the time $t = l$ (with $l \gg 1$) is thought of as a continuous and that the function $\xi(l)$ is a function of this continuous time. In this case the Shannon entropy reads

$$S(t) = - \int_{-\infty}^{\infty} dx p(x, t) \ln[p(x, t)]. \quad (6)$$

We also assume that

$$p(x, t) = \frac{1}{t^{\delta(t)}} F\left(\frac{x}{t^{\delta(t)}}\right) \quad (7)$$

and that $F(y)$ maintains its form, namely that the statistics of the process is independent of time. Let us plug Eq.(7) into Eq. (6). Using a simple algebra, we get:

$$S(\tau) = A + \delta(\tau)\tau, \quad (8)$$

where

$$A \equiv - \int_{-\infty}^{\infty} dy F(y) \ln[F(y)] \quad (9)$$

and

$$\tau \equiv \ln(t). \quad (10)$$

The assumptions made to get the result of Eq. (8) are not correct during the transition process, and consequently the DE method can be used as a reliable way to detect scaling only in the long-time limit. The DE can be used however to shed light into the regime of transition that is deeply connected with the foundation itself of statistical mechanics. According to Khinchin [15] the central limit theorem is fundamental for the realization of canonical equilibrium. As well known, a process resulting from the sum of N independent variables yields a Gaussian distribution, provided that N is large and the single variables have a probability distribution with a finite second moment. A physical process making N increase from values of the order of unity to values so large as to fit the prediction of the central limit theorem can be perceived as a transition from the microscopic to the macroscopic regime, where thermodynamics applies. If the microscopic variables do not have a finite second moment, the ordinary central limit theorem must be replaced by the generalized central limit theorem [16] and in the limiting case of $N \rightarrow \infty$ we find Lévy rather than Gauss statistics. We can generalize the point of view of Khinchin and consider also in this case the process of transition of N from small to large values as a form of transition from the microscopic to the thermodynamic regime.

Due to the nature of the DE method, the role of N is here played by the “time” t . The microscopic regime refers to the fluctuation of ξ_i and the macroscopic regime corresponds to the fluctuations of the diffusion coordinate $x(t)$. The time evolution of $\delta(t)$ towards the final value, independent of time, reflects the transition from dynamics to thermodynamics.

We shall adopt three different walking rules (see Section IV). The first two rules are characterized by an extended regime of transition from dynamics to thermodynamics. Notice that the real data available are finite, thereby producing saturation effects in the long-time regime. Consequently, the region where the ideal

scaling shows up, is an intermediate time region following the extended initial transition and preceding the long-time saturation regime. This has the effect of reducing the size of the time region that can be fruitfully used for scaling detection. As we shall see, this is the reason why the DE method must be supplemented by the use of artificial sequences. The third rule, on the contrary, yields a fast transition to the thermodynamic regime, thereby allowing us to determine the scaling by a direct use of Eq. (8), with $\delta(t)$ assuming the time independent value of the thermodynamic limit.

III. DYNAMIC MODEL

The solar flares analyzed in this paper are perceived as a sequence of events occurring at unpredictable times, t_i , with $i = 1, \dots, M$, where M is the label of the last event considered. We do not take into account the intensity of these events, which will be studied somewhere else. Thus, the most important property for us to study, is the time distribution density, $\psi(\tau)$, with τ denoting the time distance between two nearest neighbor events, $\tau_i \equiv t_{i+1} - t_i$. Let us make the assumption that the experimental analysis of the time series yields the form

$$\psi(\tau) = (\mu - 1) \frac{T^{\mu-1}}{(T + \tau)^{\mu}}. \quad (11)$$

We make the key assumption that the numbers τ_i are uncorrelated. As we shall see, the theory of this paper affords also a criterion to assess if this crucial assumption is correct or not. Under this key assumption we can build up a dynamic model that is statistically equivalent to the solar dynamics generating the sequence of the t_i 's. Let us consider the dynamic process:

$$dy/dt = \lambda y^z, \quad (12)$$

with $z > 1$. Let us imagine that the trajectory $y(t)$ moves within the interval $[0, 1]$. Let us assume also that when the trajectory reaches the right border of this interval it is injected back within this interval by means of a random selection of the initial position $y(0)$. The random selection is done by using a random number generator that assigns the same probability to the numbers of the interval $[0, 1]$. The connection between the initial condition and the exit time τ is given by

$$y(0) = [1 + (z - 1)\lambda\tau]^{-\frac{1}{z-1}}. \quad (13)$$

This leads immediately to the distribution of Eq.(11) with

$$\mu = \frac{z}{z - 1} \quad (14)$$

and

$$T = \frac{\mu - 1}{\lambda}. \quad (15)$$

We are now equipped to establish a connection with the entropy production per unit of time. Randomness here is involved at the moment of selecting the initial condition, and is characterized by an unknown amount of entropy increase, H . If $\mu > 2$, the distribution of Eq.(11) yields a finite mean waiting time

$$\langle \tau \rangle = \frac{T}{\mu - 2}. \quad (16)$$

It is evident then that the rate of entropy production per unit of time is given by

$$h_E = H \frac{(\mu - 2)}{T}. \quad (17)$$

Using the dynamic model it is possible to establish a more proper connection with the KS entropy. However, this is of no great relevance within the context of the present paper. Therefore, we limit ourselves to considering the entropy production of Eq. (17), where the subscript E stands for "external". In fact, in the picture adopted in the present paper the source of entropy production is the random selection of the numbers of the interval $[0,1]$, an action external to the process under study. It has to be pointed out that this external entropy production is subtly related to the KS entropy, which, on the contrary, is interpreted as being of internal origin [17]. This is so because the dynamical model is a map with a very sharp chaotic region that reduces to a set of zero measure, confined to the point $y = 1$, in the limiting condition where the idealized model of this section applies.

In the case $\mu < 2$ the entropy produced is proven [7] to be the following function of time:

$$S(t) \propto t^{\mu-1}. \quad (18)$$

It is evident that in the limiting case of very large time values the entropy production per unit of time vanishes, thereby implying that the condition, $\mu = 2$ is a border at which a kind of phase transition occurs. In the region $\mu > 2$ the dynamical system of Eq. (12) has an invariant distribution. In the region $\mu < 2$ the system does not have an invariant distribution [7]. From an intuitive point of view we can imagine that during the observation process the system keeps moving towards an equilibrium distribution, as a kind of Dirac delta function located at $y = 0$ [7]. The time necessary to reach this invariant distribution is infinite.

In conclusion, an infinitesimally small change from $\mu > 2$ to $\mu < 2$ would have the effect of annihilating the invariant distribution and of making the process "non-stationary." The method of analysis of this paper will allow us to assess that $\mu = 2.138 \pm 0.01$, namely, that the solar flares fluctuations are stationary, even if very close to the border with the "non-stationary" region. This result will be obtained by a direct evaluation of μ , supplemented by the adoption of the DE method. As we shall see, this conclusion is reached after settling a major problem caused by the existence of a genuine form

of non-stationary behavior, a fact that is more properly related to dynamic rules changing upon change of time. This will lead us to the final conclusion that the model of Eq. (12) is a fairly accurate way of mimicking solar flare dynamics, with $z < 2$ ($\mu > 2$). In Sections VII and VIII we shall make some conjectures on how to improve this model to take into account the time dependence of the solar flare rate.

IV. ON THREE DISTINCT PRESCRIPTIONS TO WALK

The scaling detected by the DE method is not independent of the walking rules that we adopt. The outcomes of DE method are not unique, due to the dependence of the scaling parameter δ on the walking rules, and this casts doubts on this method of analysis. However, the task of this analysis is an indirect evaluation of the waiting time distribution $\psi(\tau)$, or, equivalently, in the inverse power law case, of the index μ . If we take for granted the inverse power law structure of $\psi(\tau)$, the power index μ is unique. We adopt the following prescriptions for the random walker:

Rule No. 1. Make a jump of fixed intensity, only when you meet an event, and do it always in the same direction.

Rule No. 2. As with Rule No. 1, make a jump only when you meet an event, but do it either in the positive or negative direction according to a coin tossing prescription.

Rule No. 3. Walk at fixed interval of times, with jumps in the same direction, of intensity proportional to the time distance between two nearest-neighbor events.

Note that here we analyze the sequence $\{\tau_i\}$, where each value τ_i denotes the time distance between two nearest-neighbor flares (regarded as events). Thus, rules No. 1 and No. 2 imply that the random walker makes instantaneous jumps at the times of flare occurrence. With rule No. 3 the random walker, at times $t = 1, 2, \dots, n, \dots$, makes jumps ahead of intensity equal to the values τ_i of the sequence under study. Note that rule No. 1 is one of the two rules used in Ref. [9]. Here we use for the first time rules No. 2 and No. 3. Using the theory of Ref. [9], which, in turn, essentially rests on the generalized central limit theorem [16] and on the work of Feller [18], we obtain the following prescriptions:

$$\delta = \begin{cases} \mu - 1, & 1 < \mu < 2 \\ 1/(\mu - 1), & 2 < \mu < 3 \\ 0.5, & \mu > 3, \end{cases} \quad (19)$$

$$\delta = \begin{cases} 0.5(\mu - 1), & 1 < \mu < 2 \\ 0.5, & \mu > 2 \end{cases} \quad (20)$$

and

$$\delta = 1/(\mu - 1), \quad \mu > 1, \quad (21)$$

for rules No. 1, No. 2 and No. 3, respectively.

Fig. 1 shows clearly that the adoption of rule No. 1 alone would yield two distinct possible values for μ when δ gets values within the interval $[0.5, 1]$. However, the joint adoption of this and the other two rules settles this ambiguity. We also notice that both rule No. 1 and rule No. 2 reflect the phase-transition character of the condition $\mu = 2$, while rule No. 3, apparently, does not. However, we see that rule No. 3 for $\mu < 2$ yields a value of $\delta > 1$, namely a diffusion process faster than the ballistic diffusion. This is a consequence of the non-stationary nature of the condition $\mu < 2$.

It is important to stress that these rules imply that the numbers τ_i are not correlated. Furthermore, these rules rest on the assumption that the asymptotic limit of $\psi(\tau)$ is an inverse power law distribution with no truncation. We shall see that the DE method is sensitive to the correlation among the numbers τ_i , and that the 11-year solar cycle is responsible for that correlation. As to the truncation of the inverse power law at the large distances, this is another delicate issue worth of some comments. Laherrère and Sornette, [19], suggest that the stretched exponential family might have a theoretical motivation stronger than the power-law distribution. On the other hand, in the intermediate time region a stretched exponential is indistinguishable from a power law. The two proposed fitting functions become distinguishable one from the other in the long-time regime, which is affected by poor statistics. However, the work of Refs. [20] and [21] show that a truncation of the power law of $\psi(\tau)$ at large times yield an ultra-slow convergence to normal diffusion, with effects that are beyond the range of observation of the DE analysis, due to the data statistical limitation.

We shall see that both rule No. 1 and rule No. 2 yield a very slow transition to the scaling regime. Due to the statistical limitation of our data, the scaling regime turns out to be a relatively short time region between transition and saturation regime. Thus, we shall be forced to carry out our analysis with the help of artificial sequences with the same number of terms as the real data, by fitting the DE curves produced by the real data with the DE curves generated by the artificial sequences. The adoption of the third rule, on the contrary, yield a fast transition to the thermodynamic regime and, consequently, makes it possible to make a direct evaluation of δ . In both cases, however, the physical consequences of a possible truncation of the inverse power law are beyond our range of observation.

V. STATISTICAL ANALYSIS OF THE REAL DATA: $\psi(\tau)$ AND $\Psi(\tau)$

In this section we plan to derive the waiting time distribution $\psi(\tau)$ directly from the statistical analysis of the real data, the x-rays emitted by solar flares in the case

here under study. At first sight, one might think that a direct determination of $\psi(\tau)$ is more convenient than any indirect approach. Actually, it is not so. As mentioned in Section I, we find that the evaluation of the probability of finding no time distance larger than a given τ , denoted by $\Psi(\tau)$, defined by

$$\Psi(\tau) \equiv \int_{\tau}^{\infty} \psi(t) dt, \quad (22)$$

is more convenient than the direct evaluation of $\psi(\tau)$. In later sections we shall prove a striking property: the evaluation of μ through the DE method, an approach less direct than the evaluation of $\Psi(\tau)$, is still more efficient.

The data are a set of 7212 hard x-ray peak flaring event times obtained from the BATSE/CGRO (Burst and Transient Source Experiment aboard the Compton Gamma Ray observatory satellite) solar flare catalog list. The data is a nine-year series of events from 1991 to 2000. If the time Δt between two consecutive solar flares is expressed in seconds, the range goes from 45 to 10,000,000 seconds, as shown in Fig. 2. Fig. 3 shows the rate of solar flares per month from April 1991 to May 2000. The set of data studied here concerns a time period of 9 years, and, consequently, a large part of the whole 11-year solar cycle. Fig. 3 shows that during a large portion of this 11-year cycle the flare rate undergoes big changes, thereby significantly departing from the uniform distribution. Furthermore, it is worth remarking that, as shown by Fig. 4, the 11-year solar cycle is not a mere harmonic oscillation with the period of 11 years, but a complex dynamic process with many components.

The direct evaluation of the waiting time distribution, $\psi(\tau)$, needs the data to be distributed over many bins with the same size. When only a few data are available, the bin size cannot be too small, and, in turn, the adoption of bins of large size can produce incorrect power law indices. In proceeding with the direct evaluation of the key parameter μ , first of all, we have to adopt a proper criterion to determine the size Δ_i of the i -th bin. We note that the waiting time distribution is expected to be an inverse power law. If we adopted bins of equal size, those corresponding to large times would collect a very limited amount of data, thereby resulting in a non reliable evaluation of the frequencies. To bypass this difficulty we adopt bin sizes that are constant in the logarithmic scale. This means that $\ln(\tau_i) - \ln(\tau_{i-1})$, where τ_i and τ_{i-1} are the middle times of two consecutive bins, is constant. We define the width of the i -th bin as $\Delta = \tau_i - \tau_{i-1}$, thereby making it become an exponentially increasing function of the sequence position, so as to widely compensate for the density decrease. In this representation the probability density $\psi(\tau_i)$ is expressed by

$$\psi(\tau_i) = \frac{N_i}{N \Delta_i}, \quad (23)$$

where N is the total number of data points, N_i is number

of points located within the i -th bin, and Δ_i , as earlier said, is the width of the i -th bin.

The fitting is done by using the prescription of a power law of the type of Eq. (11)

$$\psi(\tau) = \frac{A_1}{(T + \tau)^\mu}, \quad (24)$$

with A_1 , T and μ being three independent fitting parameters. It is worth noting that the normalization condition reduces the three independent parameters to two, as made clear by Eq. (11), which is a function of only T and μ . We find it to be more convenient to adopt three independent fitting parameters, with the understood proviso that the departure of A_1 from the value $(\mu - 1)T^{\mu-1}$ can be interpreted as a way to estimate the inaccuracy of the adopted fitting procedure.

The fitting is done by using an implementation of the nonlinear least-squares (NLLS) Marquardt-Levenberg algorithm [22]. The NLLS algorithm may not give unique values for the fitting parameters. It needs initial guesses for the free parameters and the final results may change or be affected by huge errors. This fitting procedure yields: $T = 8787$, $\mu = 2.12 \pm 0.32$ and $A_1 = 31006$. The evaluated value of A_1 is not far from the value 29236 that would be required by the normalization condition. However, there are very large errors of the order of 100%, with an error on the parameter μ of the order of 15%, thereby implying $1.80 < \mu < 2.44$. This means that the result of this fitting procedure would prevent us from assessing the important question raised in Section III on whether the process is stationary or non stationary. The large error of this procedure depends upon the initial values assigned to the three fitting parameters, T , μ and A_1 , whose choice requires a more efficient criterion. It also depends on the fact that there are oscillations around the fitting curve, as clearly illustrated by Fig. 5.

As earlier mentioned several times, a more accurate fitting is obtained using the function $\Psi(\tau)$. Again we do not pay attention to the normalization constraints and we adopt the following fitting function

$$\Psi(\tau) = A_2 \left(\frac{1}{T + \tau} \right)^{\mu-1}. \quad (25)$$

As shown by Fig. 6, the fitting of the real data is now much more accurate than that of Fig. 5. The fitting parameters used are: $A_2 = 30657 \pm 16590$, $T = 8422 \pm 500$, $\mu = 2.144 \pm 0.05$. This sets on the key parameter μ the constraint $2.094 < \mu < 2.194$, which has the very attractive property of establishing the stationary nature of the dynamic model behind the solar flares fluctuations. The results of this search for μ , based on the direct evaluation of $\psi(\tau)$ and on the use of $\Psi(\tau)$, are summarized in Table I. We note that the uncertainty interval associated with the use of $\Psi(\tau)$ is contained within the wider uncertainty interval produced by the use of $\psi(\tau)$. This means that we are coming closer to the real value of μ . The width of

the uncertainty interval will be further reduced by using the DE method.

Table I

$\psi(\tau)$	$\Psi(\tau)$
$1.80 < \mu < 2.44$	$2.094 < \mu < 2.194$

VI. DIFFUSION ENTROPY OF SOLAR FLARES.

This section is devoted to the analysis of the solar flares data by means of the DE method. The final result will be given by $\mu = 2.138 \pm 0.01$, namely a value for μ even more accurate than that obtained in Section V by using $\Psi(\tau)$. We shall prove also that the DE method allows us to establish some aspects of the dynamics behind solar flares that would be overlooked by an analysis based only on the use of the waiting time distribution.

The first issue that we have to solve is how to process the data so as to apply the three walking rules of Section IV. The data accessible to us are the times $\tau_i = t_i - t_{i-1}$, with t_i and t_{i-1} denoting the time of occurrence of the i -th and the $(i-1)$ -th solar flare, respectively. However, the direct adoption of these numbers would result in technical difficulties that are bypassed by referring ourselves to the new sequence of numbers

$$\beta_j = \text{Int} \left[\frac{\Delta t_j}{\Lambda} \right] + 1, \quad (26)$$

where $\text{Int}[x]$ denotes the integer part of x . The adoption of $\Lambda = 1$ would be virtually equivalent to referring ourselves to the original sequence of numbers. However, preliminary trials with changing values of Λ led us to conclude that there are problems with the adoption of both excessively small and excessively large values of Λ . The adoption of excessively small values of Λ would make the computer analysis too slow and would require an excessively large amount of computer memory. This is the reason why we cannot use the original sequence of numbers. The adoption of excessively large values of Λ , on the other hand, would produce statistical saturation, and a consequent sub-diffusion process that would not accurately reflect the dynamics behind the data. We adopted the criterion of using the largest value of Λ compatible with negligible saturation effect. Preliminary attempts made it possible for us to assess that this convenient value is given by $\Lambda = 3600$.

After processing the data, we have to realize the three walking rules of Section IV. We note that according to the prescription of Section II, diffusion is generated by the random walker jumping at any time step. The random walker makes jumps of intensity $|\xi_i|$, ahead or backward, according to whether $\xi_i > 0$ or $\xi_i < 0$. Thus, we create a new sequence ξ_i , of 0's and 1's, with the following prescription. We consider a sequence of infinite empty sites, labeled by the integer index i , considered as a discrete time, running from $i = 1$ to $i = \infty$. We divide

this sequence into patches of width β_j . The first patch consists of the sites $i = 1, i = 2, \dots, i = \beta_1$, the second patch consists of the sites $i = \beta_1 + 1, \beta_1 + 2, \dots, \beta_1 + \beta_2$, and so on. We assign the value 0 to all the sites of the same patch but the last site. This means that the random walker walks only at the end of the patch, namely, at the occurrence time of an event. To apply rule No. 1, with the random walker always moving in the same direction, we always assign to the last site of a given patch the value of 1. To apply rule No. 2 we assign to the last site of any patch either the value 1 or the value -1, according to the coin tossing rule. The coin tossing prescription is realized by using a random number generator. To reduce the risk of artificial periodicity we create 10 different sequences, each corresponding to a different random distribution of 1's and -1's. For any sequence we run the DE method and then we make the average over the 10 resulting DE curves. To apply the rule No. 2, which will be shown in action in Section VII C, we have to identify ξ_i with β_i .

The DE results obtained applying rule No. 1 are illustrated in Fig. 7. This figure shows one of the benefits of the DE method. According to rule No. 1, we have to use the prescription of Eq. (19). The most accurate of the values of μ , discussed in Section V, is $\mu = 2.144$. This value, being smaller than 3 and larger than 2, makes us adopt the formula $\delta = 1/(\mu - 1)$, and yields the scaling parameter $\delta = 0.874$, which is the slope of the straight line of Fig. 7.

This theoretical prediction implies that the times τ_i of the sequence $\{\tau_i\}$ are not correlated with each other. In the specific case of seasonal periodicity described by harmonic oscillations, the numerical results of Ref. [8] prove that the scaling detected by the DE, as well as by other methods to detect scaling, is higher than the Brownian motion scaling $\delta = 0.5$. This is so even when there is no correlation in addition to seasonal periodicity. We eliminate this effect, by shuffling the data. The DE method can be applied to both the original sequence of β_i and to the shuffled sequence. If the DE yields two different curves, this is a proof of the fact that there is memory in the original sequence. This is an important property that cannot be revealed by the analysis of the waiting time distribution, $\psi(\tau)$. Fig. 7 shows that this is the case. In fact we see that the DE curve corresponding to the shuffled data, after the transition region at short time and before saturation, has a slope distinctly smaller than the curve referring to the non shuffled data. Furthermore, this slope is closer to the slope of the straight line corresponding to the finding of Section V, which yields $\mu = 2.144$, and, consequently, according to Eq. (19), $\delta = 0.874$. However, both shuffled and non-shuffled data yield saturation effects at a time scale of the order of $t_{sat} = 1,500$ hours. These saturation effects set limits to the accuracy of the determination of the value of μ by means of the DE method.

In Fig. 8 we illustrate the results obtained by using rule No. 2. It is remarkable that in this case the shuffled data yield, with the DE method, an entropy increase faster

(rather than slower) than the non-shuffled data. This is a consequence of the fact that in this case the deviation from ordinary diffusion, produced by time periodicity, would generate sub-diffusion rather than super-diffusion. We notice that the difference between the shuffled and non-shuffled curves is smaller than that in the case of Fig. 7 (rule No. 1) and that the saturation effects show up at later times. We thus conclude that rule No. 2 is much less sensitive to periodicities and to saturation effects than rule No. 1.

VII. A FURTHER IMPROVEMENT: USE OF ARTIFICIAL SEQUENCES

We have seen that the DE method reveals the existence of memory effects that are overlooked by the direct evaluation of the waiting time distribution. However, as pointed out in Section II and illustrated by the numerical results of Section VI, the time region where the DE method might be fruitfully used to detect scaling, is reduced to an intermediate time region, after the transition from dynamics to thermodynamics, and before the saturation effects. This has the unwanted effect of setting limitations to the accuracy of the DE method. To bypass this difficulty we generate artificial sequences with the same statistical limitations of the real data, and then we search for the parameter μ that establishes the most accurate fitting with the DE curves derived from real data.

To make this procedure as reliable as possible we proceed as follows. We assume that $\psi(\tau)$ has the form

$$\psi(\tau) = \frac{A}{(T + \tau)^\mu}, \quad (27)$$

where T and μ are our fitting parameters. The constant A is determined by the normalization condition through

$$\frac{1}{A} \equiv \int_{45}^{\infty} \frac{1}{(T + \tau)^\mu} d\tau. \quad (28)$$

The fitting parameters are made to change around the mean values established by the results of Section V which yield $\mu = 2.144 \pm 0.05$ and $T = 8422 \pm 500$. Note that in the real data no time exists with a value smaller than $\tau = 45$ sec. This is the reason why the integration in Eq. (28) is done from 45 to ∞ rather than from 0 to ∞ . The number of data available to us are 7211. Thus we produce 7211 values of τ_i , according to the prescription

$$\tau_i = \left[\frac{1}{(T + 45)^{\mu-1}} - \frac{(\mu - 1) y_i}{A} \right] - T, \quad (29)$$

with the number y_i randomly selected in the interval $[0, 1]$. It is straightforward to prove that the resulting distribution of τ_i is the same as that of Eq. (27) and fits the condition of Eq. (28). At this stage we are ready to

compare the DE curves generated by the artificial data to the DE curves generated by the real data, using both rule No. 1 and rule No. 2. The comparison is made with the DE curves corresponding to shuffled data, since the artificial sequences are generated without correlation among the numbers τ_i .

Let us discuss first the results concerning rule No. 1. These results are illustrated in Figs. 9. In Fig. 9a we show the effect of changing μ in the interval $[2.094, 2.194]$, with $T = 8422$ and in Fig. 9b we show the effect of changing T in the interval $[7922, 8922]$, with $\mu = 2.144$. We see that the DE curves of the artificial sequences fluctuate within an error strip containing the DE curve of the real data. The size of this error strip increases upon change of time and we see that the spreading caused by the change of T is much smaller than that caused by the change of μ . From a qualitative point of view, the results concerning rule No. 2, shown in Figs. 10a and 10b, are very similar.

A. A more accurate measurement of μ .

We have seen that the area of the T-error strip is significantly smaller than that of the μ -error strip, at least five times smaller. Therefore, we can improve the accuracy of μ by assigning to T a fixed value and looking for the value of μ ensuring the best fitting of the real data. We assign to T the value of 8422, and we proceed with the search for the best fitting. The results are illustrated in Figs. 11a and 11b. The result concerning rule No. 1 is good, as seen in Fig. 11a. As expected, Fig. 11b shows that the result concerning rule No. 2 is even better, and we think that it can be judged to be excellent. This extremely accurate result is due to the DE curve of the artificial sequence coinciding with the DE curve of real data over the wide range of 1000 hours of diffusion. On the basis of this excellent fitting, we conclude that

$$\mu = 2.138 \pm 0.01. \quad (30)$$

B. Non shuffled data and an artificial sequence with suitable memory.

In Section VI, we have noticed that the result of the DE analysis depends on whether the real data are shuffled or not. We think that in the original data there are signs of the 11-year solar cycle and other subcycles. This makes it harder to establish a connection between the scaling δ and the power index μ . However, if our conclusion that $\mu = 2.138 \pm 0.01$ is correct, it should be possible to fit the DE curve of the non-shuffled original data with no further change of the fitting parameters T and μ , provided that we sort the artificial sequence in such a way as to mimic the solar periodicity. Rather than doing that with a model, for instance a suitable modulation of the parameter λ of Eq. (12), we proceed in a more direct

way, according to the following procedure. Let us call R_i and A_i the i -th numbers of the real and artificial sequence used in subsection A, respectively. The i -th number of the sorted artificial sequence is denoted by S_i . The subscript i ranges from 1 to N . The number S_1 is fixed by selecting from the set of A_i 's the number that is closest to R_1 , this being, let us say, $A_{j(1)}$. We thus set $S_1 = A_{j(1)}$. The number $A_{j(1)}$ is eliminated from the artificial sequence. Then, we move to R_2 and from the set of the remaining $N-1$ numbers of the artificial sequence we select the closest one to it, this being, let us say, $A_{j(2)}$. We proceed with the same criterion until we exhaust all the numbers of the artificial sequence. It is evident that the adoption of this procedure assigns to the artificial data a time order reflecting the complex dynamics illustrated by Figs. 2 and 3.

At this stage, we evaluate the corresponding DE curve and we compare it to the DE curve generated by the non-shuffled real data. As earlier mentioned, the sorted artificial data are the same as those used to produce the excellent fitting of the DE curves derived from the shuffled original data. Thus, the fitting parameters are the same as those used for Figs. 11. We illustrate the new result in Figs. 12, which show that the fitting accuracy is as good as (and for rule No. 1 even slightly better than) the fitting of Figs. 11. This is a very remarkable result since Figs. 7 and 8 show that shuffling the data produces a significant effect. Thus, Figs. 11 and 12 prove that the memory of the data is totally under our control.

C. Third rule in action.

According to Lepreti, Carbone and Veltri [23] the waiting time distribution $\psi(\tau)$ is already Lévy. This would imply that the adoption of the third rule yields an infinitely fast transition from dynamics to thermodynamics. This is so because Lévy distribution is stable and the convolution between two distinct Lévy distributions is a Lévy distribution [16]. According to our analysis, $\psi(\tau)$ is a shifted inverse power law. It is plausible that the difference between the shifted power law distribution of Fig. 5 and the Lévy distribution of Ref. [23] is small. Consequently, the transition to thermodynamics is expected to be very fast. This expectation is confirmed by the numerical results illustrated in Fig. 13. The transition to the scaling regime is so fast that it is possible to detect a wide regime of linear dependence of the entropy on $\log(l)$, which allows us to derive for μ the value $\mu = 2.138$, in total agreement with the conclusion of the earlier analysis done by means of rules No. 1 and No. 2. We see that in this case the memory of the non-shuffled data yields a δ slightly larger than the scaling parameter of the shuffled data. The adoption of rule No. 3 implies a statistical accuracy smaller than that of the other two rules, due to fact there is no limitation to the jumps intensities, thereby decreasing the number of particles located in the

same cell. This has the effect of making the evaluation of p_i and consequently that of the entropy less accurate. However, this disadvantage is widely compensated by the emergence of a much more extended scaling region that yields as a result a value of μ fully confirming that of the other two rules.

VIII. CONCLUDING REMARKS

We see that the uncertainty on the value of μ for solar flares has been significantly reduced. The current literature, if we give the same credit to all the authors, yields values of μ ranging from 3 to 1.7. We provide the compelling conclusion that $\mu = 2.138 \pm 0.01$. However, this is not the main result of his paper. We think that this paper shows that the DE method is a remarkably accurate technique of analysis that goes much beyond the direct evaluation of the waiting time distribution $\psi(\tau)$. This is so because complex processes are characterized by two different kinds of memory. The memory of first kind is the main object of the research work done in the field of the Science of Complexity. To make clear the nature of this kind of memory, let us recall [24] that a Markov master equation, namely a stochastic process without memory, is characterized by a waiting time distribution $\psi(\tau)$ with an exponential form, thereby implying memory for a marked deviation from the exponential condition. This is why the search for an inverse power law distribution with a finite value of μ (the exponential distribution means $\mu = \infty$) can be interpreted as a search for memory. This is the memory of the first kind, to which the prescriptions of Ref. [9] are referred to. For real data, in addition to this form of memory, another type of memory might be present, denoted by us as memory of the second type, under the form of correlation among the values τ_i . In this paper we have seen that this second form of memory is given, in this case, by the 11-year solar periodicity. It is possible that this form of additional memory is present in many other complex processes for different reasons. It is also evident that it is difficult, or perhaps impossible to reveal this form of additional memory by means of the direct evaluation of $\psi(\tau)$. This paper proves that joint use of the direct evaluation of $\psi(\tau)$ (or of $\Psi(\tau)$) and of the DE method is a very useful supplement to the ordinary technique, and that it can be profitably used to shed light on the dynamics behind the time series generated by complex processes.

This paper yields a convincing conclusion concerning the distinction between two possible forms of non-stationary behavior. As pointed out in Section III, the claim that the waiting time distribution $\psi(\tau)$ has the form of Eq. (11) is equivalent to assuming that the dynamics of the flaring process is driven by the model of Eq. (12) with the assumption that the trajectories are injected back randomly. This is a stationary model that in the case where $z > 2$, ($\mu > 2$), would be incompati-

ble with the existence of an invariant distribution [7] and consequently with “thermodynamic equilibrium”. The inaccuracy of the analyses done by the earlier work in this field would prevent us from distinguishing this form of non-stationary behavior from a genuinely form of non-stationary behavior. By genuinely non-stationary behavior, we mean the existence of rules changing with time. This form of genuinely non-stationary behavior might be modelled, for instance, by assuming that the parameter λ of Eq. (12) is time dependent. If we make the assumption that the time dependence of λ has a period of 11 years, and we make our analysis over a period of time that is not much larger than this time period, as we have done, then the process must be perceived as being genuinely non stationary. Our analysis is so accurate as to rule out the former form of non-stationary behavior and to detect significant effects stemming from the latter, or, equivalently, from the existence of the memory of the second type.

In this paper we do not take side with either the proponents of self-organized criticality [25] or with those of turbulence [3,4]. The dynamical model of Section III is inspired by the models of turbulence, but we mainly use it to generate artificial sequences mimicking the real ones with no claim that it is an exhaustive picture of the dynamics behind solar flares. The fitting of Fig. 6 seems as good as the fitting of Fig. 1 of Ref. [23]. However, our analysis does not rest only on the waiting time distribution. In a very recent paper Wheatland [26] criticized the work of Ref. [23] as being based on the assumption that rate of solar flares is constant. This is not so, as shown by Fig. 3. On the other hand, modelling the time dependence of this rate is not easy, since it does not correspond only to a 11-year periodic motion but to a much more complex condition, as illustrated in Fig. 4. In fact, this figure shows that there are many other components in action. This is the reason why we decided to mimic the time dependence of the solar flare rate sorting the artificial sequence in the way described in Section VII B. We found that this yields a fitting with the real data as good as the fitting between the DE curve produced by the artificial sequence, with no sorting induced memory, and the DE curve produced by the shuffled real data. This is, in our opinion, a strong indication that the value of $\mu = 2.138$ is a genuine property of real data. On the other hand, the dynamical model of Section III can also be adapted to reproducing the modulated Poisson process advocated by Wheatland [26]. This is left as a subject of future investigation. Even in this case, the role of the DE analysis is expected to be crucial, and the result is expected to strongly depend on whether the modulation process involves randomness or only quasi-periodicity.

In our notation, the power index found by the authors of Ref. [23] is $\mu = 2.38$, a value that turns out to be compatible with the uncertainty interval associated to the determination of μ by means of the direct evaluation of $\psi(\tau)$. Our analysis establishes a connection with Lévy statistics, in accordance again with the conclusions

of Ref. [23]. However, we adopt a perspective that is different from that of the authors of Ref. [23]. Our diffusion process reaches the Lévy regime after the process of transition from dynamics to thermodynamics that has been discussed in detail in the earlier sections. This process is very fast if the rule No. 3 is adopted, but it is not infinitely fast as in the perspective of the authors of Ref. [23] who assume the waiting time distribution $\psi(\tau)$ to obey already the Lévy statistics. It is worth pointing out that the perspective adopted in this paper makes it possible to take into account the time dependence of the solar flare rate. We do not rule out the possibility that $\psi(\tau)$ is a stretched exponential [19]. In fact, a stretched exponential would not conflict with the attainment of Lévy statistics in the long-time limit of the diffusion process. Although a truncation of $\psi(\tau)$ at large values of τ generates a finite second moment, and consequently Gaussian statistics in the long-time limit, the transition to the conventional thermodynamic regime is ultra slow [20]. It is known [21] that a much earlier transition to Lévy statistics occurs and that the Lévy regime lasts for a very extended period of time. The transition to the Gaussian regime probably takes place at times much larger than the saturation time, and might be made visible only in the ideal case of infinitely large sequences.

Acknowledgements: we thank the BATSE/CGRO team, NASA/Goddard Space Center, Greenbelt, Md, for generously providing the data.

- [12] K.Hu, P. Ch. Ivanov, Z. Chen, P. Carpena, H.E. Stanley, Phys. Rev. E **64**, 011114 (2001).
- [13] C. Beck, F. Schlögl, *Thermodynamics of chaotic systems*, Cambridge University Press, Cambridge (1993).
- [14] J.R. Dorfman, *An Introduction to Chaos in Nonequilibrium Statistical Mechanics*, Cambridge University Press, Cambridge (1999).
- [15] A.I. Khinchin, *Mathematical Foundations of Statistical Mechanics*, Dover Publications, Inc. New York (1949).
- [16] B.V. Gnedenko, A.N. Kolmogorov, *Limit Distributions for Sum of Independent Random Variables*, Addison Wesley, Reading (1954).
- [17] P. Grigolini, M. Pala and L. Palatella, Phys. Lett. A **285**, 49 (2001).
- [18] W. Feller, Trans. Am. Math. Soc. **67**, 98 (1949).
- [19] J. Laherrère and D. Sornette, Eur. Phys. J. B **2**, 525 (1998).
- [20] R. N. Mantegna and H. E. Stanley Phys. Rev. Lett. **73**, 2946 (1994)
- [21] E. Floriani, R. Mannella, P. Grigolini, Phys Rev E **52**, 5910 (1995).
- [22] W. H. Press and others, *Numerical Recipes in C*, Cambridge University Press, Cambridge (1992).
- [23] F. Lepreti, V. Carbone, and P. Veltri, Astrophys. J. **536**, L133 (2001).
- [24] D. Bedeaux, K. Lakatos Lindenber and K.E. Shuler, J. Math. Phys. **12**, 2166 (1971).
- [25] M.S. Wheatland, P.A. Sturrock, and J.M. McTiernan, Astrophys. J. **509**, 448 (1998).
- [26] M. S. Wheatland, arXiv:astro-ph/0107147.

-
- [1] E.N. Parker, Astrophys. J. **330**, 474 (1988); E.N. Parker, Sol. Phys. **121**, 271 (1989).
 - [2] R.P. Lin, R.A. Schwarz, S.R. Kane, R.M. Pelling, and K.C. Hurley, Astrophys. J. **283**, 421 (1984); S. Sturrock, P. Kaufmann, P.L. Moore, and D.F. Smith, Sol. Phys. **94**, 341 (1984); N.B. Crosby, M. J. Aschwanden, and B.R. Dennis, Sol. Phys. **143**, 275 (1993).
 - [3] G. Boffetta, V. Carbone, P. Giuliani, P. Veltri, and A. Vulpiani, Phys. Rev. Lett. **83**, 4662 (1999).
 - [4] P. Giuliani, V. Carbone, P. Veltri, G. Boffetta, A. Vulpiani, Physica A **280**, 75 (2000).
 - [5] M. S. Wheatland, Astrophys. J. **536** L 109 (2000).
 - [6] M. Annunziato, P. Grigolini, Phys. Letters A **269**, 31 (2000).
 - [7] M. Ignaccolo, P. Grigolini, A. Rosa, Rev. E **64**, 026210 (2001).
 - [8] M. Scafetta, P. Hamilton, P. Grigolini, Fractals **9**, 193 (2001).
 - [9] P. Grigolini, L. Palatella, G. Raffaelli, in press on Fractals, **cond-mat/0104166**.
 - [10] N. Scafetta, V. Latora, P. Grigolini, submitted to PRL, **cond-mat/0105041**.
 - [11] C.-K. Peng, S.V. Buldyrev, S. Havlin, M. Simons, H. E. Stanley, A. L. Goldberger, Phys. Rev E **49**, 1685 (1994).

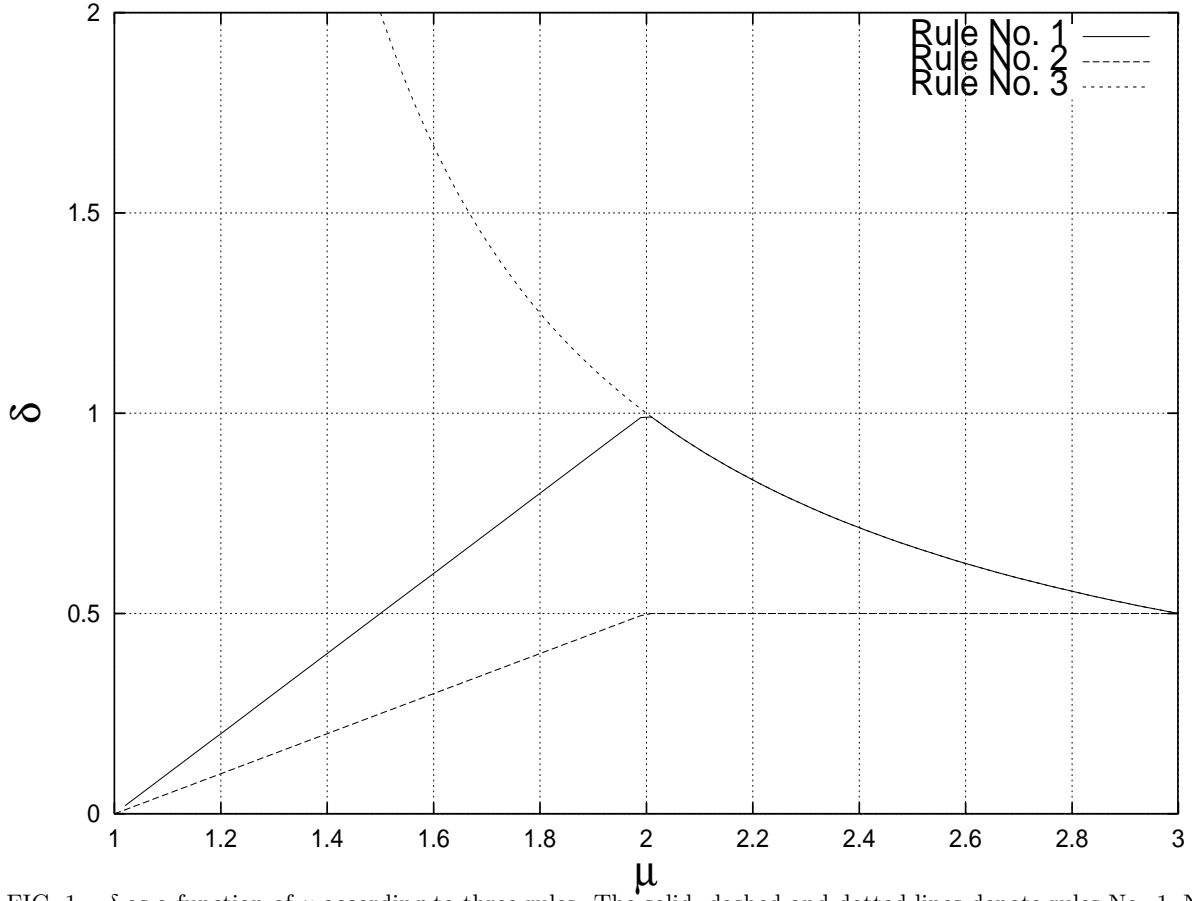


FIG. 1. δ as a function of μ according to three rules. The solid, dashed and dotted lines denote rules No. 1, No. 2 and No. 3, respectively.

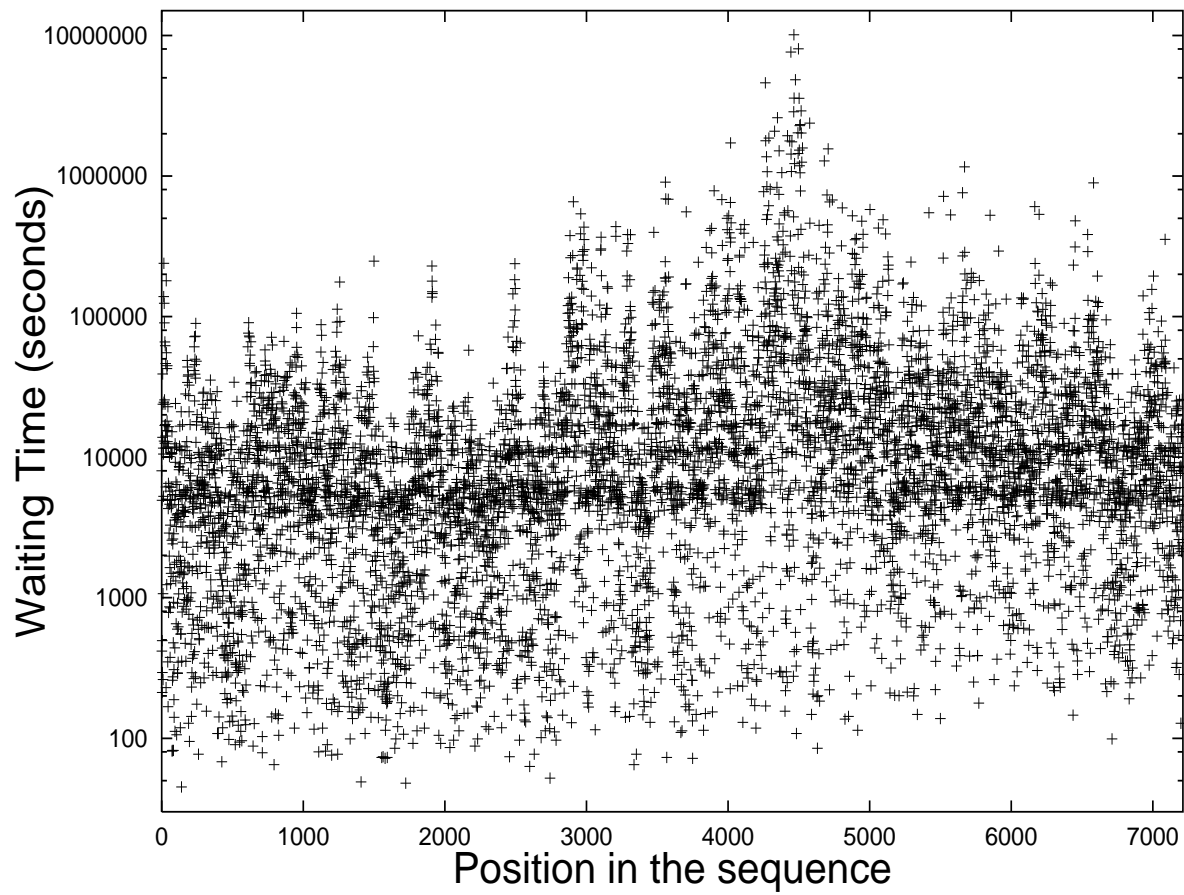


FIG. 2. The original sequence of the solar flares waiting times. Note the logarithmic scale of ordinates.

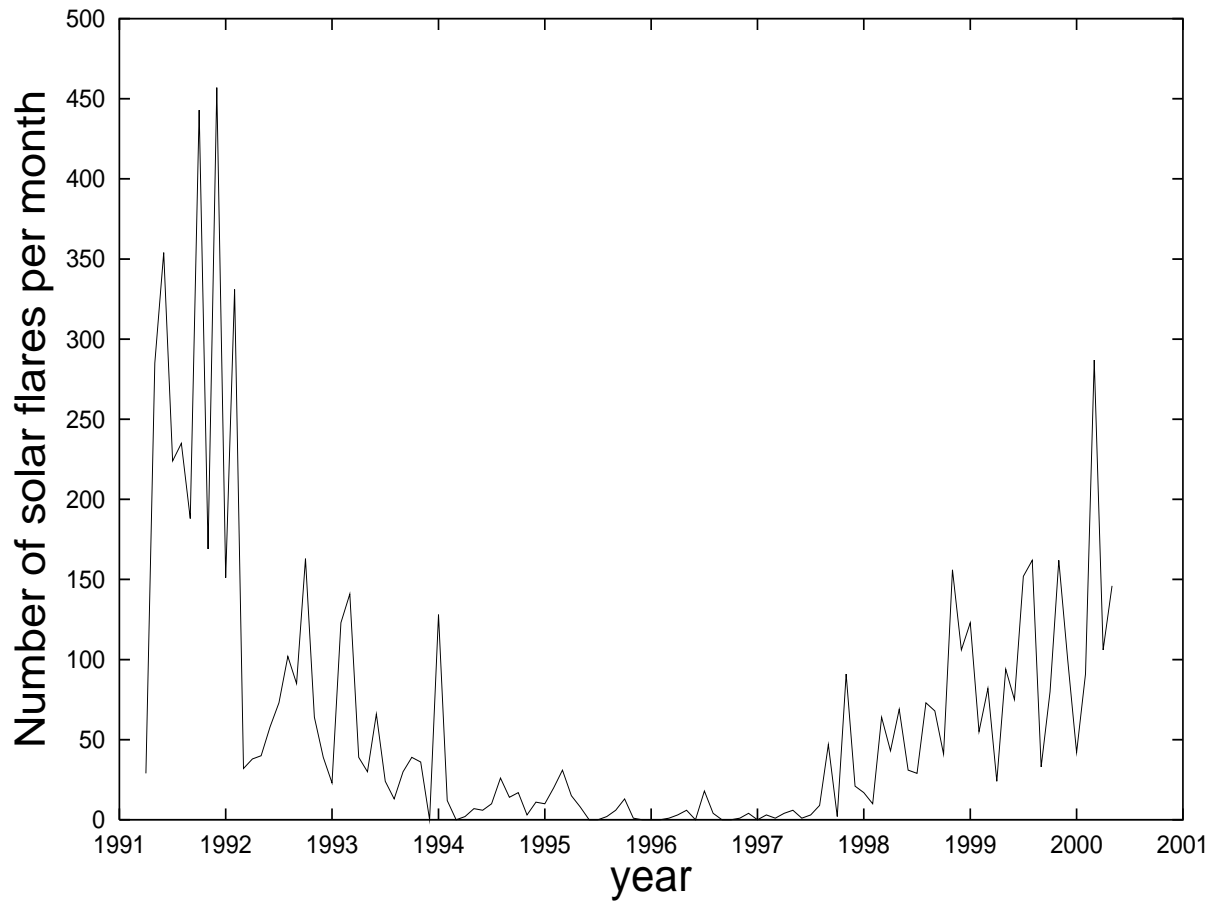


FIG. 3. Number of solar flares per month from April 1991 to May 2000.

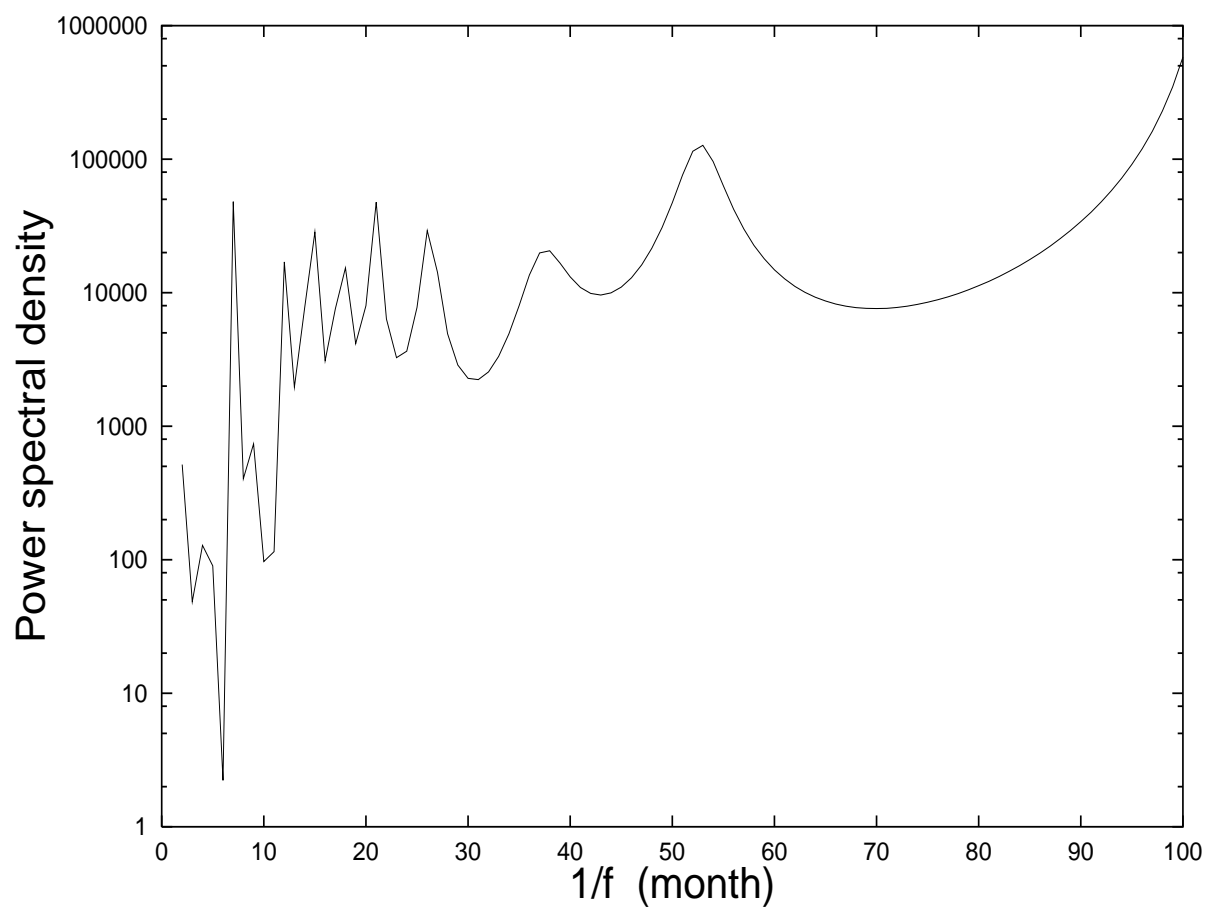


FIG. 4. The solid curve was obtained by using the maximum entropy method [22].

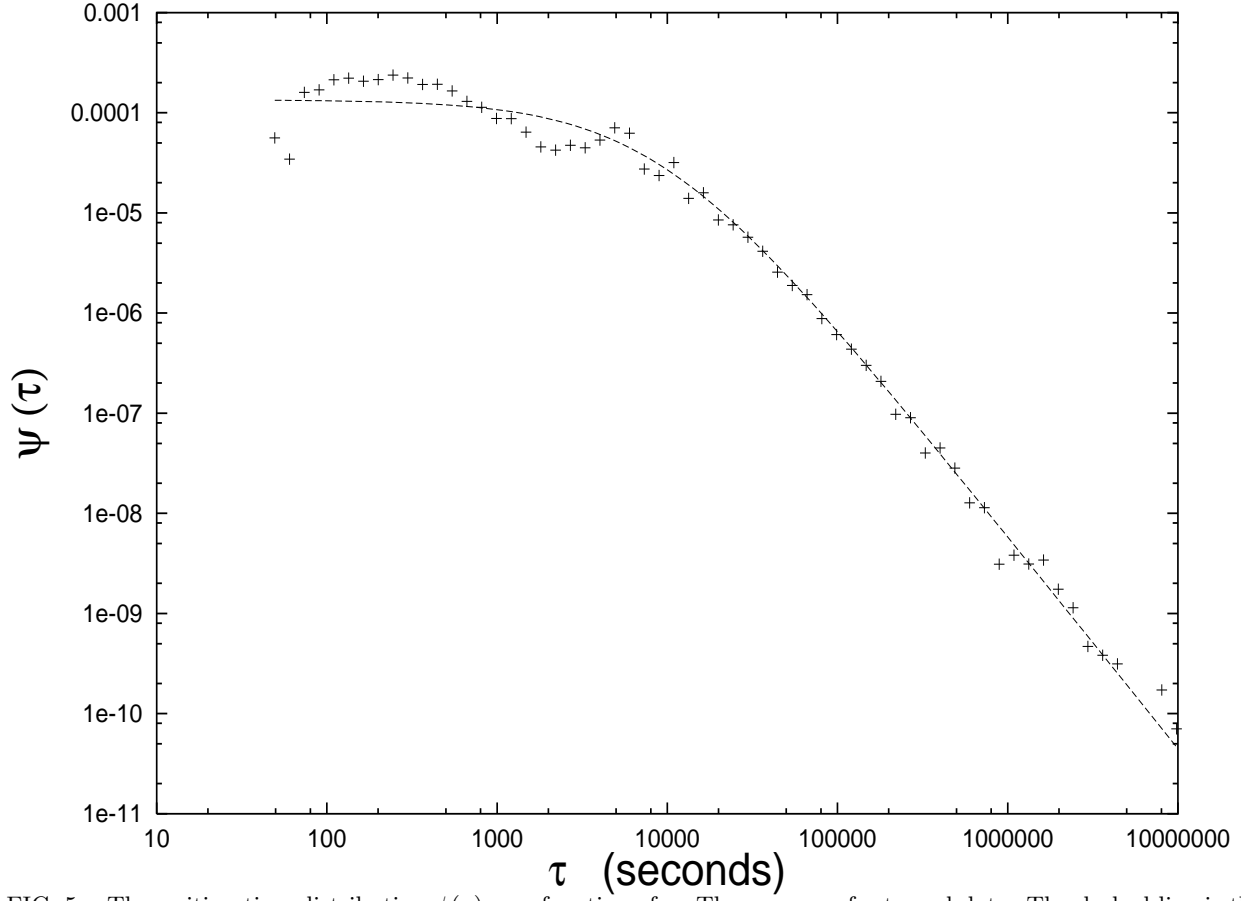


FIG. 5. The waiting time distribution $\psi(\tau)$ as a function of τ . The crosses refer to real data. The dashed line is the fitting function of Eq. (24) with $A_1 = 31006$, $T = 8787$ and $\mu = 2.12$.

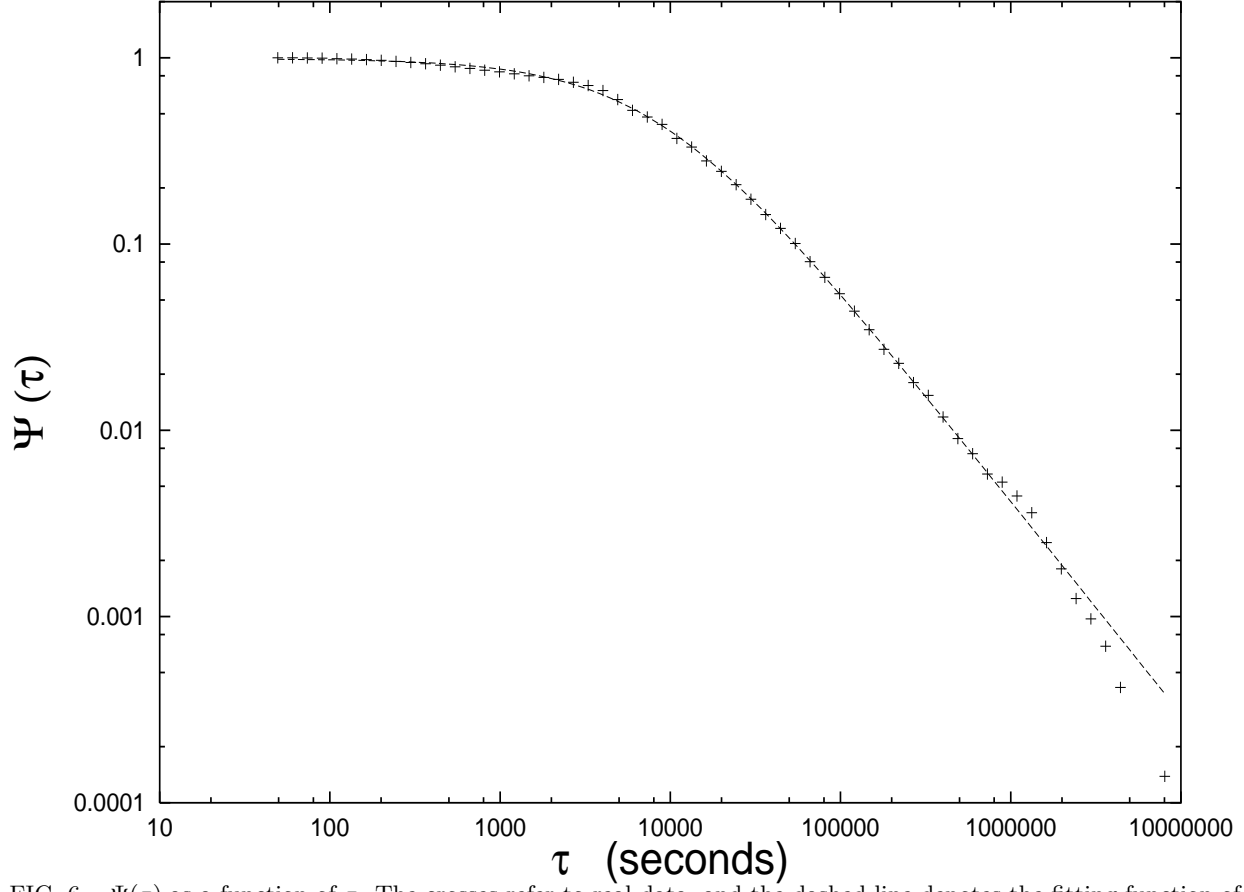


FIG. 6. $\Psi(\tau)$ as a function of τ . The crosses refer to real data, and the dashed line denotes the fitting function of Eq. (25) with $A_2 = 30567$, $T = 8422$ and $\mu = 2.144$.

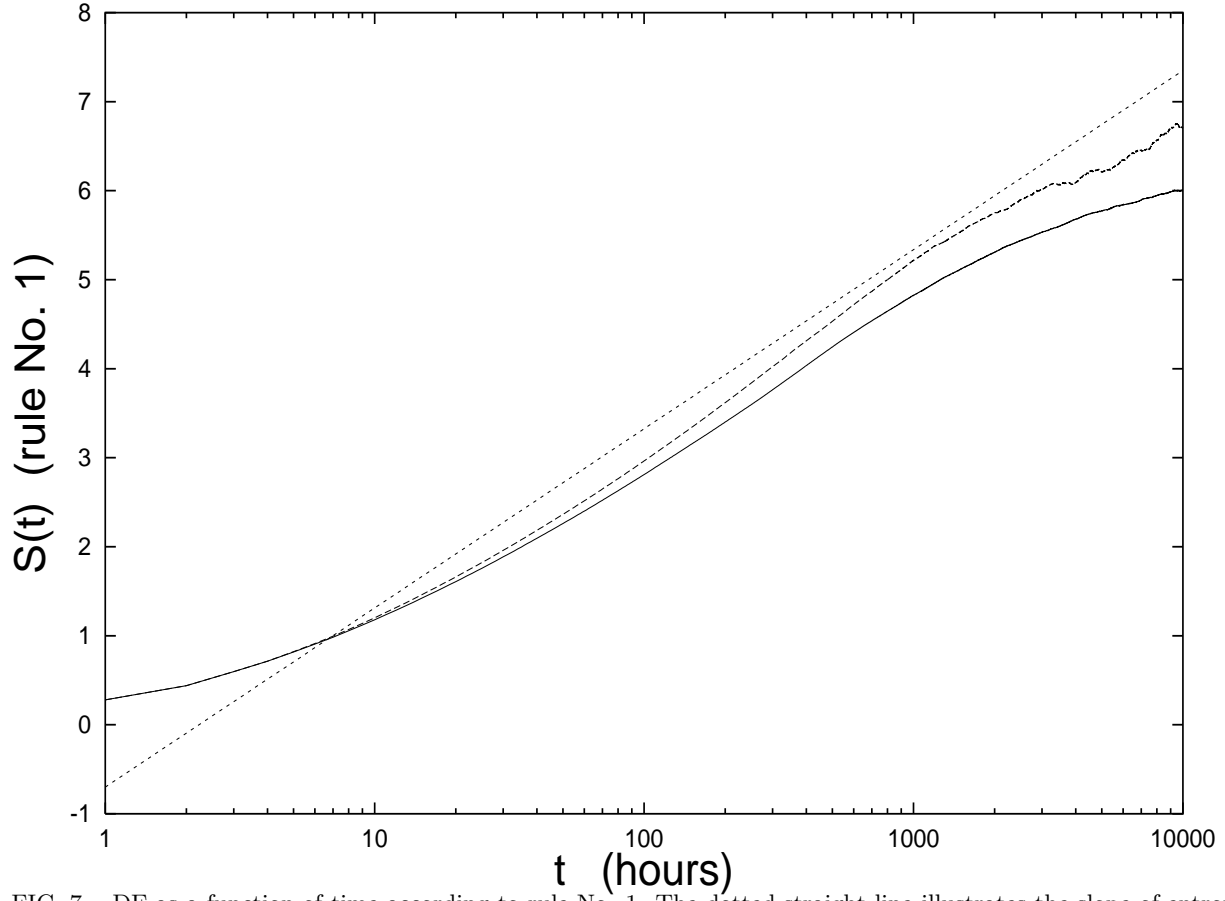


FIG. 7. DE as a function of time according to rule No. 1. The dotted straight line illustrates the slope of entropy increase corresponding to $\mu = 2.144$, and $\delta = 0.874$, which is the best value of μ afforded by the analysis of Section V. The dashed line is the DE curve generated by the non-shuffled real data. The solid line is the DE curve generated by the shuffled real data.

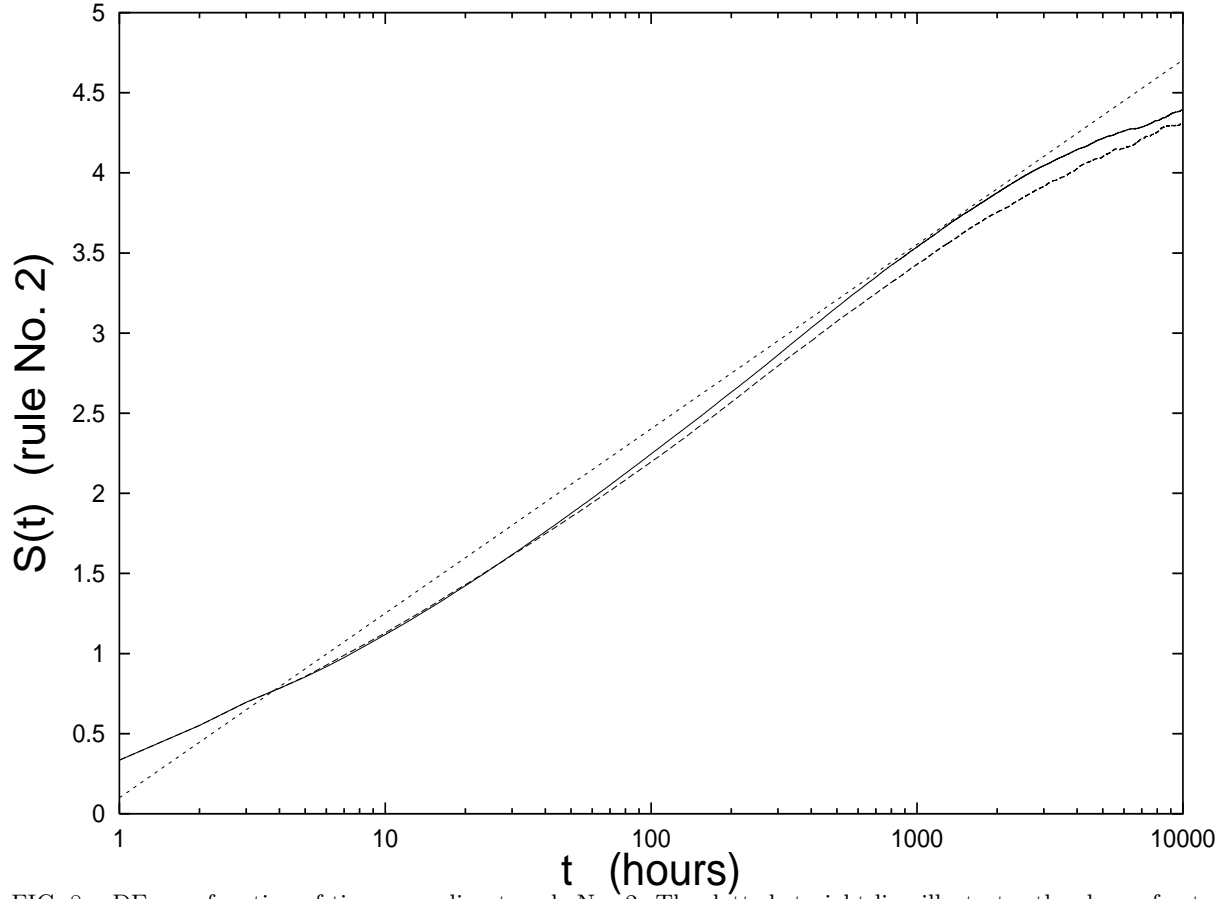


FIG. 8. DE as a function of time according to rule No. 2. The dotted straight line illustrates the slope of entropy increase corresponding to $\mu = 2.144$, $\delta = 0.5$, which is the best value of μ afforded by the analysis of Section V. The dashed line is the DE curve generated by the non-shuffled real data. The solid line is the DE curve generated by the shuffled real data.

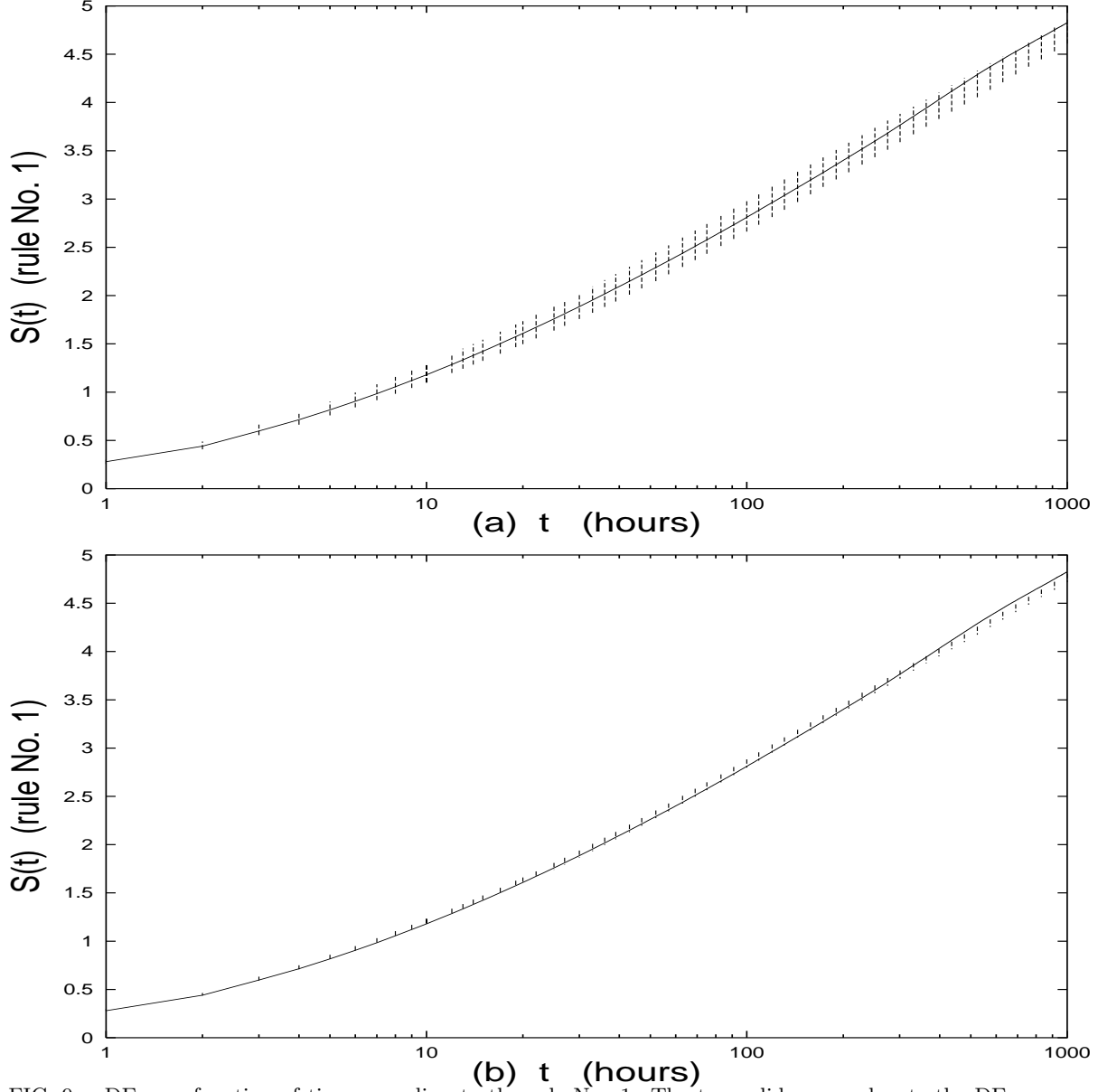


FIG. 9. DE as a function of time according to the rule No. 1. The two solid curves denote the DE curve corresponding to the shuffled real data. (a) The vertical bars indicate the changes of the DE curves resulting from the artificial sequences described in the text with $T = 8422$ and μ moving in the interval $[2.094, 2.194]$. (b) The vertical bars indicate the changes of the DE curves resulting from artificial sequences described in the text with $\mu = 2.144$, and T moving in the interval $[7922, 8922]$.

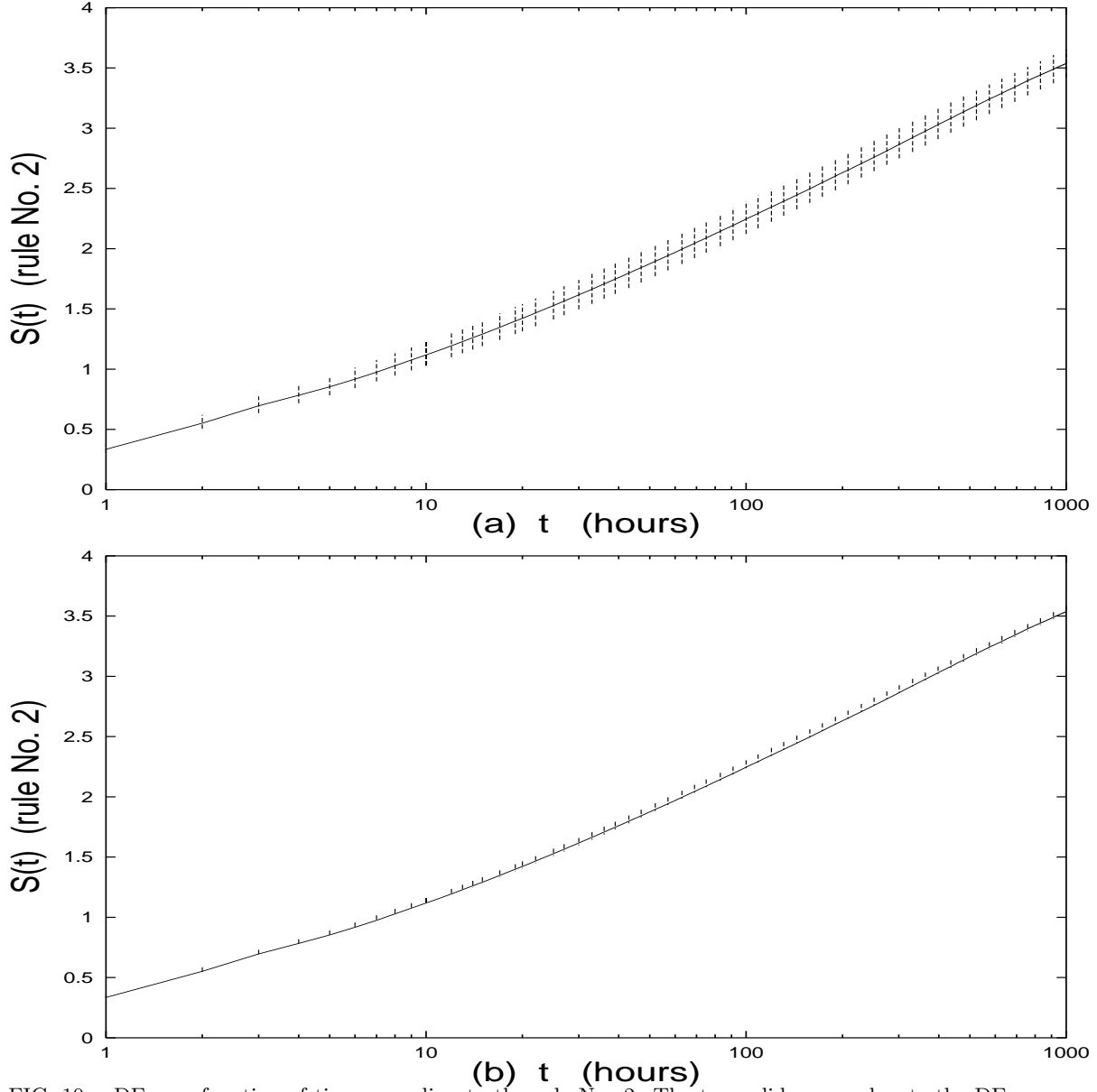


FIG. 10. DE as a function of time according to the rule No. 2. The two solid curves denote the DE curve corresponding to the shuffled real data. (a) The vertical bars indicate the changes of the DE curves resulting from the artificial sequences described in the text with $T = 8422$ and μ moving in the interval $[2.094, 2.294]$. (b) The vertical bars indicate the changes of the DE curves resulting from artificial sequences described in the text with $\mu = 2.144$, and T moving in the interval $[7922, 9922]$.

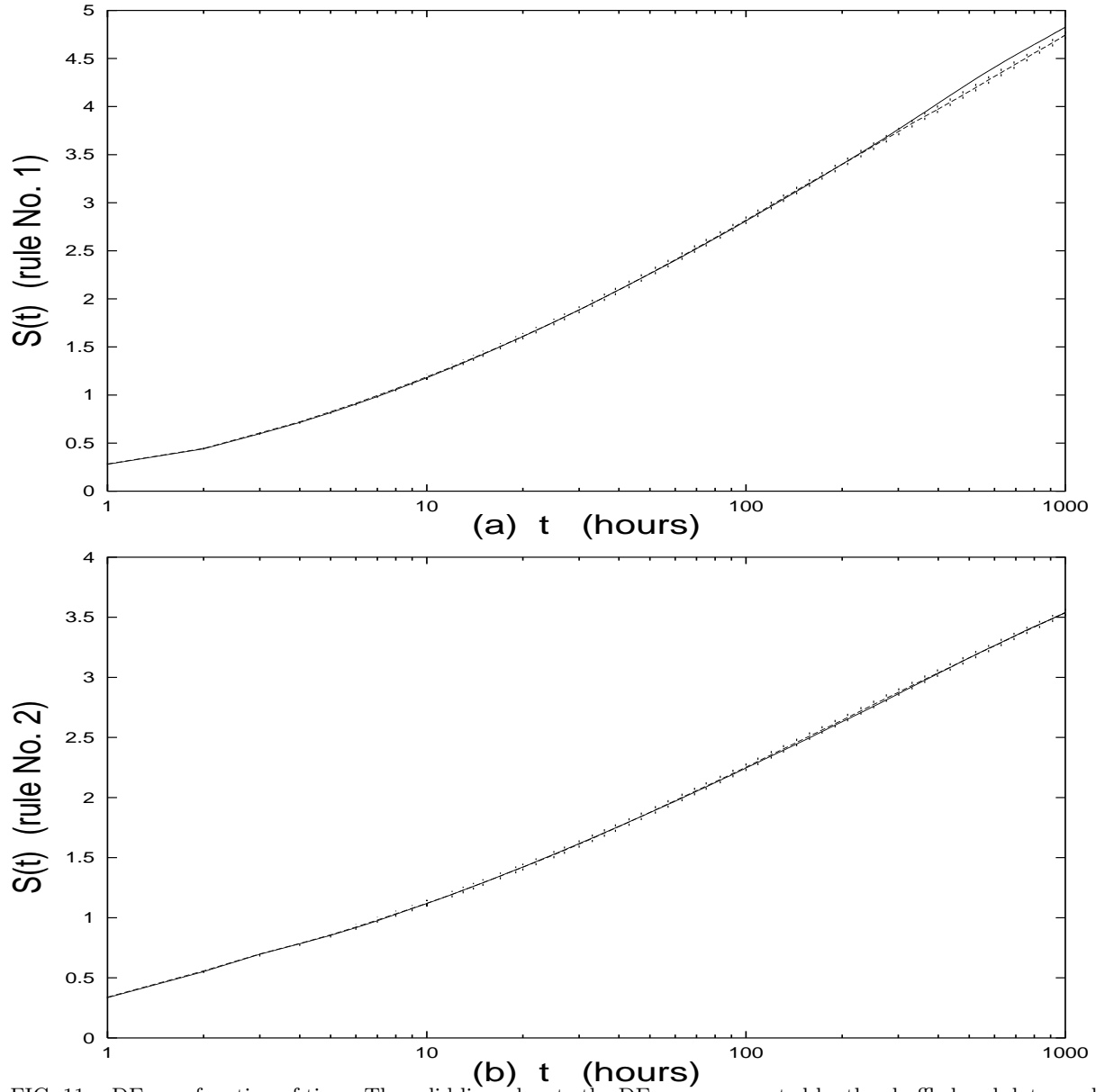


FIG. 11. DE as a function of time. The solid lines denote the DE curve generated by the shuffled real data, and the dashed lines, which almost coincide with the solid lines, denote the DE curves resulting from the artificial sequence with $\mu = 2.138$ and $T = 8422$. (a) Rule No. 1. (b) Rule No. 2.

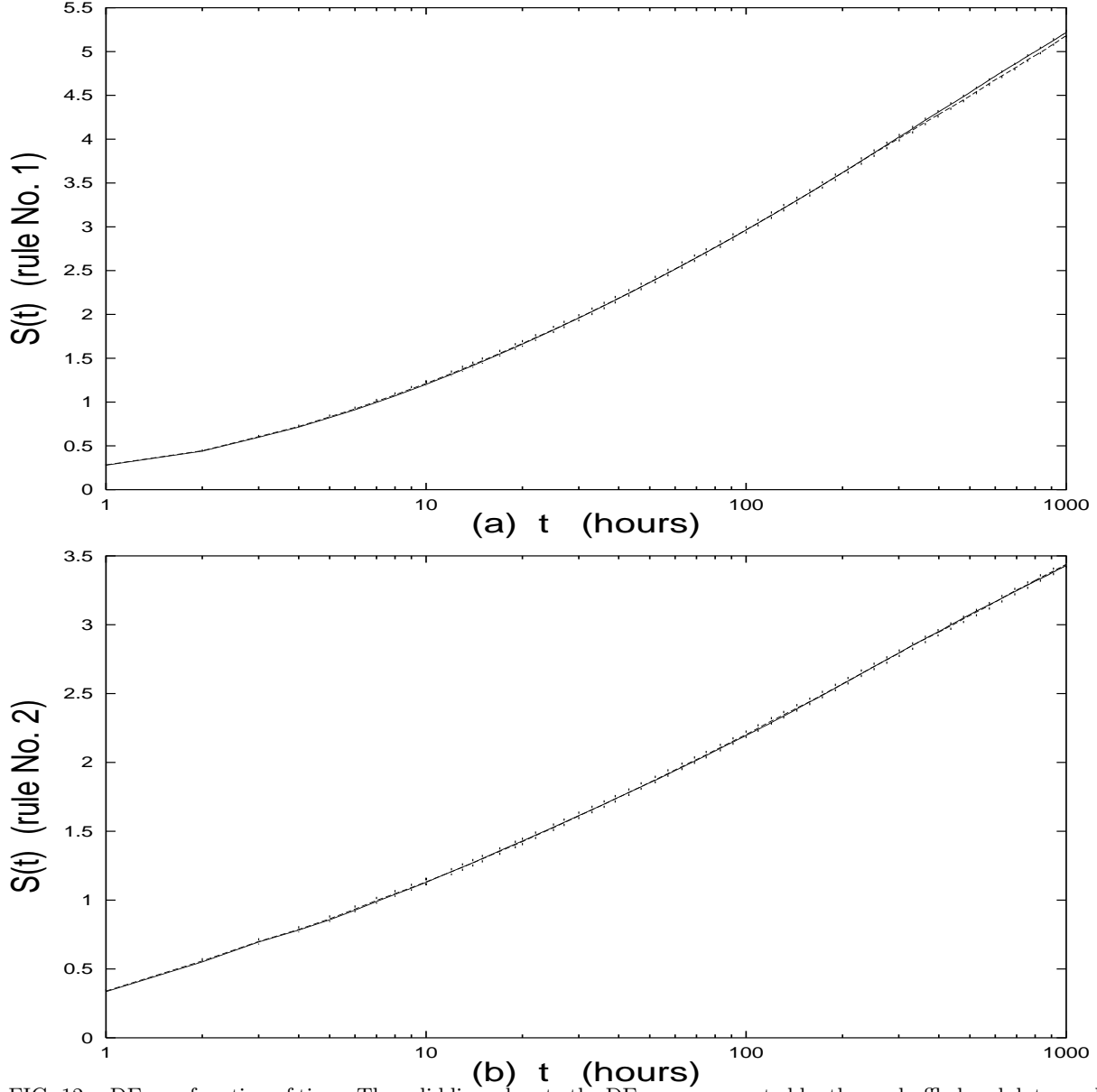


FIG. 12. DE as a function of time. The solid lines denote the DE curve generated by the unshuffled real data, and the dashed lines, which almost coincide with the solid lines, denote the DE curves resulting from the artificial sequence with $\mu = 2.138$ and $T = 8422$ with a modulation mimicking the influence of the 11-years solar cycle. (a) Rule No. 1. (b) Rule No. 2.

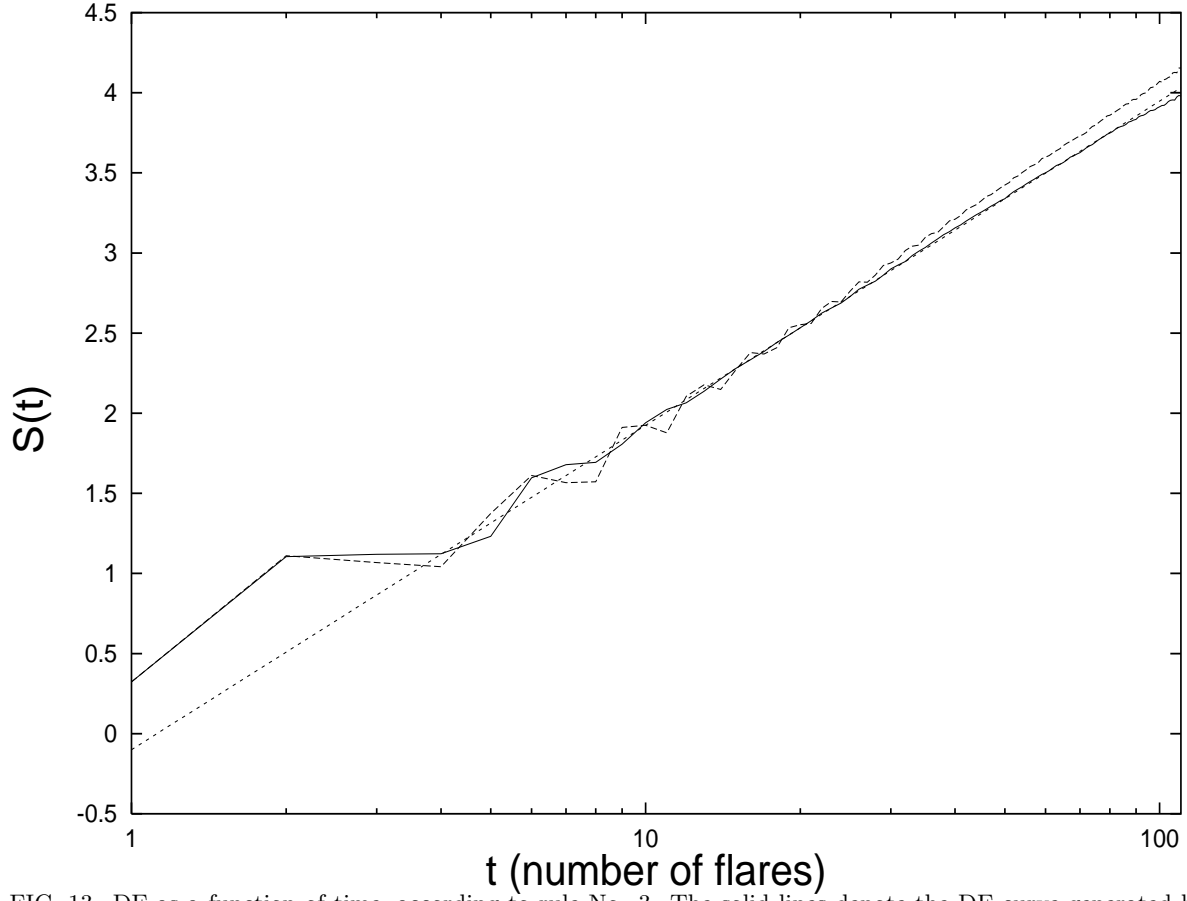


FIG. 13. DE as a function of time, according to rule No. 3. The solid lines denote the DE curve generated by the shuffled real data. The dotted straight line illustrates the slope of entropy increase, $\delta = 0.879$, which corresponds to $\mu = 2.138$. The dashed line denotes the DE curve resulting from the unshuffled real data. Note the superdiffusion of the unshuffled real data DE due to the memory in the original signal.